Wafer-level MOCVD growth of AlGaN/GaN-on-Si HEMT structures with ultra-high room temperature 2DEG mobility

Cite as: AIP Advances **6**, 115016 (2016); https://doi.org/10.1063/1.4967816
Submitted: 03 September 2016 . Accepted: 01 November 2016 . Published Online: 29 November 2016

Xiaoqing Xu, Jiebin Zhong, Hongyun So, Aras Norvilas, Christof Sommerhalter, Debbie G. Senesky, and Mary Tang

Wafer-level MOCVD growth of AlGaN/GaN-on-Si HEMT structures with ultra-high room temperature 2DEG mobility

Xiaoqing Xu,[1,a] Jiebin Zhong,[2] Hongyun So,[1] Aras Norvilas,[2]
Christof Sommerhalter,[2] Debbie G. Senesky,[1] and Mary Tang[1]
[1]*Stanford University, Stanford, California 94305, USA*
[2]*AIXTRON Inc., Sunnyvale, California 94089, USA*

(Received 3 September 2016; accepted 1 November 2016; published online 9 November 2016)

In this work, we investigate the influence of growth temperature, impurity concentration, and metal contact structure on the uniformity and two-dimensional electron gas (2DEG) properties of AlGaN/GaN high electron mobility transistor (HEMT) structure grown by metal-organic chemical vapor deposition (MOCVD) on 4-inch Si substrate. High uniformity of 2DEG mobility (standard deviation down to 0.72%) across the radius of the 4-inch wafer has been achieved, and 2DEG mobility up to 1740.3 $cm^2/V{\cdot}s$ at room temperature has been realized at low C and O impurity concentrations due to reduced ionized impurity scattering. The 2DEG mobility is further enhanced to 2161.4 $cm^2/V{\cdot}s$ which is comparable to the highest value reported to date when the contact structure is switched from a square to a cross pattern due to reduced piezoelectric scattering at lower residual strain. This work provides constructive insights and promising results to the field of wafer-scale fabrication of AlGaN/GaN HEMT on Si. [http://dx.doi.org/10.1063/1.4967816]

I. INTRODUCTION

The high growth quality and high throughput capabilities of metal-organic chemical vapor deposition (MOCVD) have enhanced and propelled research of III-nitride in power electronics, optoelectronics, timing references, high frequency applications, and harsh environment sensors.[1–11] One of the most important applications is in the fabrication of AlGaN/GaN high electron mobility transistor (HEMT) which utilizes a two-dimensional electron gas (2DEG) layer formed at the interface of GaN and AlGaN. The properties of HEMTs are dependent on the electron mobility and the sheet carrier density of the 2DEG layer. The main factors influencing AlGaN/GaN 2DEG concentration and mobility are: Al% in the AlGaN barrier,[12–14] AlGaN barrier thickness,[12–14] AlN spacer thickness,[12,13] GaN cap thickness,[15] and the impurity level[16–18] especially C% in the GaN layer, all dependent on the growth temperature and its distribution. A deeper understanding of the effects of these parameters could lead to dramatic improvements in the 2DEG mobility and its uniformity.

Based on the moderate range of these coupled parameters, the HEMT structure grown in this work was designed as follows: 4-inch Si(111) substrate (p-type, highly doped, resistivity <0.005 Ω·cm) with AlN/$Al_{0.8}Ga_{0.2}N$/$Al_{0.5}Ga_{0.5}N$/$Al_{0.2}Ga_{0.8}N$/GaN as buffer layers, and ~1 nm AlN spacer/30 nm $Al_{0.25}Ga_{0.75}N$ barrier/3 nm GaN cap. In this work, we focus on three aspects: 1. The uniformity of 2DEG mobility across 4-inch wafer, which is a combined effect of Al% and thickness distributions of the AlGaN barrier, AlN spacer and GaN cap thickness distributions, and C% distribution in the GaN layer, all closely related with the growth temperature and its distribution; 2. Influence of C and O impurity level on the 2DEG mobility; 3. Influence of contact structure on the 2DEG performance.

[a]Author to whom correspondence should be addressed. E-mail: steelxu@stanford.edu.

High mobility is useful for high-frequency electronic devices and high uniformity ensures consistency among different devices.

II. EXPERIMENTS

Wafer-level AlGaN/GaN-on-Si sample growth was achieved using an MOCVD reactor (AIXTRON CCS® 3x2) with a 4-inch susceptor. The HEMT structure growth started with two in-situ baking steps of the substrate at ~1050 °C: 5 min baking in pure hydrogen to remove Si native oxide and surface adsorption, followed by 10 min baking with the addition of Silane to protect Si surface. Then AlN was grown with 15 sec ammonium pre-flow, followed by a low temperature AlN growth at 1020~1030 °C and a high temperature AlN growth at 1120~1130 °C with a total thickness of 284 nm. The three $Al_xGa_{1-x}N$ (x=0.8, 0.5, 0.2 respectively) layers were grown at 1080~1090 °C with a thickness of 280 nm, 345 nm, 530 nm respectively. A 1.25μm-thick GaN layer was then grown at 1040~1060 °C. Finally, an AlN spacer of 1 nm, an $Al_{0.25}Ga_{0.75}N$ barrier of 30nm and a GaN cap of 3 nm were grown at ~1035 °C. All the temperatures mentioned here are true temperature of sample surface measured by EpiTT in-situ pyrometer. Sample A, B, and C were grown in the same conditions except that sample B was grown after the reactor had been exposed to some C and O contaminated experiments. The photoluminescence (PL) mapping and wafer thickness mapping were measured by Nanometrics Inc. Scanning electron microscopy (SEM) image was taken with an FEI XL30 Sirion SEM, and X-ray diffraction (XRD) pattern was measured by a PANalytical X'Pert PRO XRD system. Secondary ion mass spectroscopy (SIMS) of impurity concentration was carried out by a Cameca NanoSIMS 50L system. All Hall effect measurements, room temperature or temperature dependent measurements, were performed using an H50 Hall Effect Controller and a K2000 Temperature Controller.

III. RESULTS AND DISCUSSIONS

A. Influence of growth temperature on Al%

Although the five parameters, Al% and thickness distributions in the AlGaN barrier, AlN spacer and GaN cap thickness distributions, C% in the GaN layer, are all dependent on the growth temperature and its distribution, it is challenging and destructive to precisely determine the thickness distribution of such thin layers (1~30nm) and the C impurity elemental mapping of low concentration (down to $1x10^{16}$ cm^{-3}). The Al% distribution, however, can be determined nondestructively by PL mapping, and thus could be an indication of the growth temperature distribution and a benchmark of all the five parameters.

To test the growth temperature dependence of Al%, three AlGaN/AlN/Si testing samples were grown at a true temperature of 1000 °C, 1040 °C, and 1080 °C, respectively. Figs. 1(a) to 1(c) show the PL composition mappings of the three testing samples, and Fig. 1(d) shows the measured Al% as a function of growth temperature, indicating that the Al% is highly dependent on the growth temperature variation. The results show that, at the normal growth temperature range of 1000 to 1080°C, 1°C increase in growth temperature (on the wafer surface) results in an increase of Al composition approximately by 0.24%. Therefore, the Al% distribution is a good indicator of the growth temperature distribution, thus the uniformity of 2DEG performance can be tuned by the uniformity of Al% in the AlGaN barrier.

B. High uniformity of 2DEG mobility achieved on 4-inch wafer

There are three heating zones in the MOCVD reactor (AIXTRON CCS® 3x2). Due to the strain variation and the wafer bow development as the film layers are grown, it is much harder to control the uniformity of the full HEMT structure than the simple AlGaN/AlN/Si test structure. Fig. 2(a) shows the SEM cross section and Fig. 2(b) is the XRD pattern of our HEMT structure. The films are smooth and exhibit sharp interfaces between different layers and distinct XRD peaks, indicating high quality of grown films. A further measurement by AFM discloses an RSM of 0.13 nm in a 1μm x 1μm area and 0.822 nm in a 10 μm x 10 μm area of the GaN film surface (not shown here). By precisely

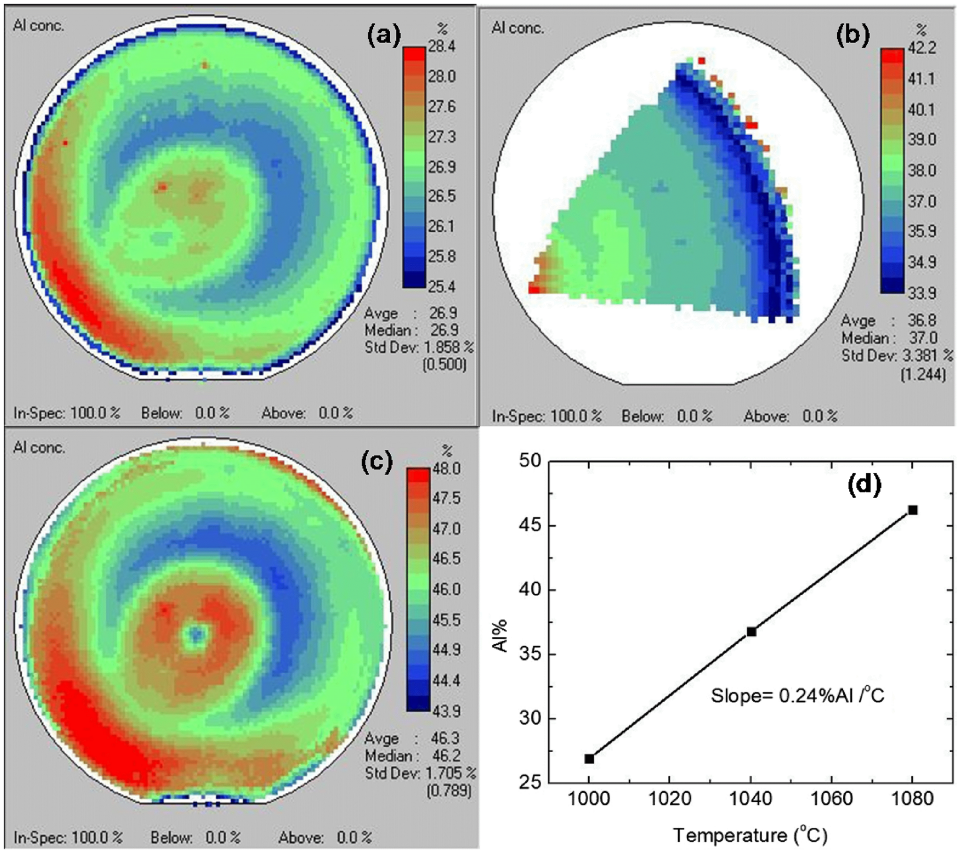

FIG. 1. PL mapping of AlGaN/AlN/Si testing structures grown at (a) 1000 °C, (b) 1040 °C, and (c) 1080 °C, respectively, (d) The growth temperature dependence of Al%, resulting in 0.24%Al/°C.

controlling the temperature settings of three heating zones in the reactor, we have obtained uniform HEMT stack (average thickness ~ 2.76 μm), in terms of Al% in the $Al_{0.25}Ga_{0.75}N$ barrier (standard deviation in percentage unit (stdev%)=2.4%) and thickness of the full GaN-on-Si HEMT structure (stdev%=3.2%), as disclosed by PL composition mapping in Fig. 2(c) and thickness mapping in Fig. 2(d), respectively. The average thickness of 2.76 μm matches pretty well with the total thickness of 2.70 μm from SEM measurement (see Fig. 2(a)). To test the uniformity of 2DEG mobility, the as-grown 4-inch wafer of HEMT structure was diced into pieces of 1 cm x 1 cm and four metal contacts were made at the corners of each piece. The metal layers are 20 nm Ti/100 nm Al/40 nm Pt/80 nm Au from bottom to top, deposited with an E-Beam evaporator. Hall measurement was done on five pieces across the radius of the 4-inch wafer. Each piece was measured twice and the average value was taken into final calculation for standard deviation. The measured results are listed in Table I. The 2DEG mobility exhibits a high uniformity with standard deviation down to 0.72% (at the average room temperature mobility of 1213.6 $cm^2/V{\cdot}s$) across the radius of the 4-inch wafer.

C. Influence of C and O impurity level on the 2DEG mobility

To investigate the effect of impurity level and contact structure on the 2DEG performance of AlGaN/GaN HEMT structure, the 2DEG properties of samples with different C and O concentrations (samples A and B) and with different contact structures (samples A and C) are compared in Fig. 3. The C and O impurity incorporation in the vicinity of the 2DEG channel can severely affect the 2DEG performance[16–18] especially when the concentration is higher than $1x10^{17}cm^{-3}$. Fig. 3(a) compares the SIMS data of Ga, C and O for samples A and B (square structure). The SIMS depth profiles were measured along all the epitaxial layers by a NanoSIMS with Cs ions as the primary ion beam. It should be noted that the interfaces between the layers are not very sharp due to the fact

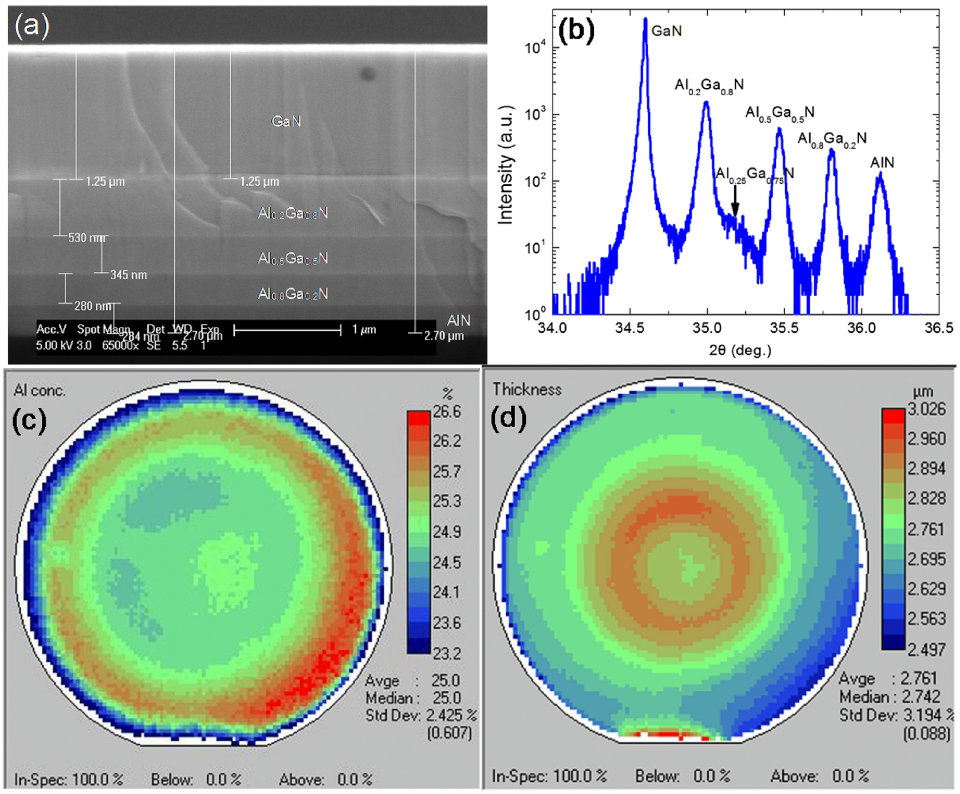

FIG. 2. (a) SEM cross section and (b) XRD pattern of the HEMT structure; (c) the PL mapping of the $Al_xGa_{1-x}N$ barrier and (d) the thickness mapping of the full HEMT structure.

of low depth resolution of NanoSIMS (i.e., instrument limitation) although high lateral resolution of 50 nm. The ultra-high C and O signals at the surface are considered a combined effect of surface molecules adsorption and instable ion yields, thus can be disregarded. Despite of the limitations of the measurement, sample B obviously exhibits higher C and O signals in all the epitaxial layers. Compared with the growth temperature profile in Fig. 3(b), it is found that the C concentration in the stack decreases as growth temperature increases, while the O concentration is almost independent of growth temperature. The measured electron mobility, sheet carrier density, and sheet resistance are summarized in Table II. It should be noted that as high as 1740.3 $cm^2/V{\cdot}s$ electron mobility was achieved at room temperature on sample A compared to sample B that has relatively higher C and O levels. The lower mobility of sample B can be explained by enhanced trapping effect and ionized impurity scattering at higher impurities incorporation.[16] It is also found that sample B has higher electron density than sample A, indicating that the dominant impurity in sample B is O other than C because O is a donor while C is an acceptor in GaN. C might be introduced into the sample because of lower growth temperature, lower reactor pressure, or evaporation from graphite susceptor and graphite carrier wafer used to hold piece samples, while O might be from the impurities in the precursor or O adsorption in the reactor as a result of the outgas from O-containing substrate (quartz wafer, for example) during other experiments. Therefore, to obtain high 2DEG mobility, growth temperature of the 2DEG channel needs to be high enough[16] and reactor condition including reactor pressure, pretreatment, and de-contamination processes needs to be controlled to reduce C and O incorporation.

D. Influence of contact structure on the 2DEG performance

Unlike samples A and B which have a square structure, sample C was fabricated into a cross structure to relieve the residual strain, thus to test the effect of piezoelectric scattering on 2DEG performance. The schematics of the two different Hall contact structures are shown in Fig. 3(c), and the

TABLE I. Measured 2DEG mobility of five samples across the radius of 4-inch wafer.

	#1	#2	#3	#4	#5	Average(cm^2/V·s)	Stdev (%)
μ1 (cm^2/V·s)	1205.7	1218.1	1217.8	1206.4	1230.6	–	–
μ2 (cm^2/V·s)	1210.5	1207.7	1206.6	1206.4	1226.2	–	–
μ (cm^2/V·s)	1208.1	1212.9	1212.2	1206.4	1228.4	1213.6	0.72

room temperature 2DEG properties are compared in Table II. It should be noted that sample C exhibits an ultra-high 2DEG mobility at room temperature (2161.4 cm^2/V·s) due to reduced piezoelectric scattering[19–21] at lower residual strain of the cross structure. This mobility is higher than most room temperature 2DEG mobilities of similar AlGaN/GaN heterostructures[22–25] and is comparable to the highest value of 2150 cm^2/V·s reported to date.[26] This ultra-high room temperature mobility is beneficial to high-frequency electronic devices in room temperature application. The residual strain in the AlGaN barrier of sample A is considered tensile due to a higher sheet carrier density than sample C.[27,28] To further verify the effect of impurity level and contact structure, temperature dependent Hall measurement was conducted for samples A, B, and C respectively from 80 K to 300 K, as shown in Fig. 3(d). Sample B with high C and O impurity level has lower mobility than sample A in the whole temperature range and shows a gentler slope especially at low temperature region (≤ 100K), indicating that the temperature independent impurity scattering[19–21] dominates the transport property of sample B. On the other hand, sample C in a cross structure reduces the piezoelectric scattering[19–21] from residual tensile strain in AlGaN/GaN heterostructure, resulting in a higher mobility and gentler slope than sample A at low temperature region (≤ 100K). In other words, piezoelectric scattering plays an important role in the transport property of 2DEG when there is a large residual strain.

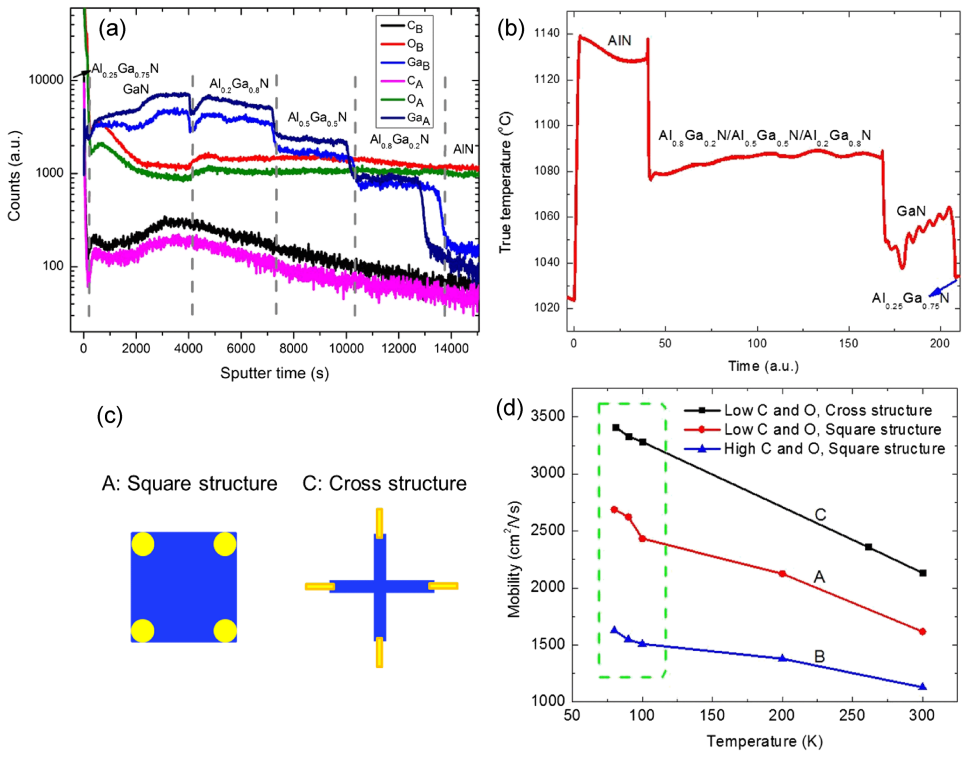

FIG. 3. (a) SIMS depth profiles of C, O and Ga in samples A and B. Ga is used as a reference signal to distinguish different layers; (b) Sample surface true temperature profile measured by in-situ EpiTT pyrometer during the HEMT growth process; (c) Schematics of the two Hall contact structures (samples A and B: Square structure; sample C: Cross structure); (d) Temperature-dependent 2DEG mobility of samples A, B, and C measured from 80 K to 300 K.

TABLE II. 2DEG performances of samples with different C and O concentrations (A and B) and with different contact structures (A and C).

	Structure	Mobility (cm^2/Vs)	Sheet Carrier Density (cm^{-2})	Sheet Resistance (ohm/cm^2)
A	Square	1740.3	9.3368E+12	384.13
B	Square	1224.6	1.2902E+13	395.04
C	Cross	2161.4	7.1593E+12	403.38

IV. CONCLUSION

In conclusion, we have demonstrated high uniformity of 2DEG mobility with standard deviation as low as 0.72% across the radius of the 4-inch GaN-on-Si HEMT wafer, and up to 1740.3 and 2161.4 $cm^2/V{\cdot}s$ 2DEG room-temperature mobility was achieved for a square contact structure and a cross contact structure, respectively. The dominant factors, growth temperature, impurity level and contact structure, on 2DEG performance and uniformity are deeply investigated and understood: AlGaN barrier composition is very sensitive to growth temperature, every 0.24% Al composition increment in the barrier corresponding to 1°C growth temperature shift on the wafer surface, thus the uniformity of 2DEG performance can be tuned by the uniformity of Al composition; high concentration of C and O impurities highly degrade the 2DEG mobility; the cross contact structure reduces piezoelectric scattering from residual tensile strain in AlGaN/GaN heterostructure which reduces the 2DEG mobility and simultaneously increases polarization induced sheet carrier density.

ACKNOWLEDGMENTS

The authors thank Dr. Zhiqiang Li and Torsten Stoll from Nanometrics for the measurement of PL mapping and thickness mapping, Chuck Hitzman from Stanford Nano Shared Facility for NanoSIMS measurement, Caitlin Chapin, Minmin Hou, Seonghyun Paik, Jieyang Jia, Ateeq Suria, and Sam Falkenhagen for process support.

This work was performed in part in the nano@Stanford labs, which are supported by the National Science Foundation as part of the National Nanotechnology Coordinated Infrastructure under award ECCS -1542152. The work was conducted at the MOCVD lab of Stanford Nanofabrication Facility (SNF), and Stanford Nano Shared Facilities (SNSF).

[1] T. Chung, J. Limb, J.-H. Ryou, W. Lee, P. Li, D. Yoo, X.-B. Zhang, S.-C. Shen, R. D. Dupuis, D. Keogh, P. Asbeck, B. Chukung, M. Feng, D. Zakharov, and Z. Lilienthal-Weber, J. Electron. Mater. **35**, 695–700 (2006).
[2] M. Pan, X. Gao, D. Gorka, M. Oliver, and S. Guo, CS MANTECH Conference, April 23rd - 26th, 2012, Boston, Massachusetts, USA.
[3] Z. J. Liu, T. Huang, J. Ma, C. Liu, and K. M. Lau, IEEE Electron Device Lett. **35**, 330–332 (2014).
[4] E. Gaubas, T. Ceponis, E. Kuokstis, D. Meskauskaite, J. Pavlov, and I. Reklaitis, Materials **9**, 293 (2016).
[5] J. Ran, X. Wang, G. Hu, J. Wang, J. Li, C. Wang, Y. Zeng, and J. Li, Microelectron. J. **37**, 583–585 (2006).
[6] H. So and D. G. Senesky, Appl. Phys. Lett. **108**, 012104 (2016).
[7] M. Wakui, R. Ito, H. Sameshima, F.-R. Hu, and K. Hane, Transducers 2009, June 21-25, 2009, Denver, CO, USA.
[8] S. Hu, S. Liu, Z. Zhang, H. Yan, Z. Gan, and H. Fang, J.Cryst. Growth **415**, 72–77 (2015).
[9] H. So and D. G. Senesky, IEEE Sen. J. **16**, 3633–3639 (2016).
[10] O. Jani, C. Honsberg, Y. Huang, J.-O. Song, I. Ferguson, G. Namkoong, E. Trybus, A. Doolittle, and S. Kurtz, *Conference Record of the IEEE Photovoltaic Specialists Conference*, 1:20–25, June 2006.
[11] H. So and D. G. Senesky, J. Phys. D: Appl. Phys. **49**, 285109 (2016).
[12] K. Abgaryan, I. Mutigullin, and D. Reviznikov, Phys. Status Solidi C **12**, 1376–1382 (2015).
[13] T. R. Lenka and A. K. Panda, Indian J. Pure Appl. Phys. **49**, 416–422 (2011).
[14] G. Y. Zhao, H. Ishikawa, T. Egawa, T. Jimbo, and M. Umeno, Jpn. J. Appl. Phys. **39**, 1035–1038 (2000).
[15] A. Asgari, M. Kalafi, and L. Faraone, Physica E **25**, 431–437 (2005).
[16] J.-T. Chen, U. Forsberg, and E. Janzen, Appl. Phys. Lett. **102**, 193506 (2013).
[17] M. Huber, M. Silvestri, L. Knuuttila, G. Pozzovivo, A. Andreev, A. Kadashchuk, A. Bonanni, and A. Lundskog, Appl. Phys. Lett. **107**, 032106 (2015).
[18] M. Tapajna, R. J. T. Simms, Y. Pei, U. K. Mishra, and M. Kuball, IEEE Electron Device Lett. **31**, 662–664 (2010).
[19] L. Hsu and W. Walukiewicz, Phys. Rev. B **56**, 1520 (1997).
[20] S. B. Lisesivdin, A. Yildiz, N. Balkan, M. Kasap, S. Ozcelik, and E. Ozbay, J. Appl. Phys. **108**, 013712 (2010).
[21] S. Gökden, Physica E **23**, 19 (2004).
[22] S. Ardali, G. Atmaca, S. B. Lisesivdin, T. Malin, V. Mansurov, K. Zhuravlev, and E. Tiras, Phys. Status Solidi B **252**, 1960–1965 (2015).

[23] I. Lee, Y. Kim, Y. Chang, J. Shin, T. Jang, and S. Jang, J. Korean Phys. Soc. **66**, 61–64 (2015).
[24] O. Katz, A. Horn, G. Bahir, and J. Salzman, IEEE Trans. Electron Dev. **50**, 2002 (2003).
[25] S. Kaun, M. Wong, U. Mishra, and J. Speck, Appl. Phys. Lett. **100**, 262102 (2012).
[26] J. Cheng, X. Yang, L. Sang, L. Guo, J. Zhang, J. Wang, C. He, L. Zhang, M. Wang, F. Xu, N. Tang, Z. Qin, X. Wang, and B. Shen, Sci. Rep. **6**, 23020 (2016).
[27] O. Ambacher, Acta. Phys. Pol. A **98**, 195 (2000).
[28] O. Ambacher, J. Smart, J. R. Shealy, N. G. Weimann, K. Chu, M. Murphy, W. J. Schaff, L. F. Eastman, R. Dimitrov, L. Wittmer, M. Stutzmann, W. Rieger and J. Hilsenbeck, J. Appl. Phys. **85**, 3222 (1999).